American Journal of Transplantation 2015; XX: 1–7
Wiley Periodicals Inc.

doi: 10.1111/ajt.13429

Brief Communication

Fluorodeoxyglucose F^{18} Positron Emission Tomography Coupled With Computed Tomography in Suspected Acute Renal Allograft Rejection

P. Lovinfosse[1,†], L. Weekers[2,†], C. Bonvoisin[2], C. Bovy[2,3], S. Grosch[2,3], J.-M. Krzesinski[2,4], R. Hustinx[1] and F. Jouret[2,4,*]

[1]*Division of Nuclear Medicine, Department of Medical Physics, University of Liège Hospital, Liège, Belgium*
[2]*Division of Nephrology, Department of Internal Medicine, University of Liège Hospital, Liège, Belgium*
[3]*Division of Renal Pathology, Unilab, University of Liège Hospital, Liège, Belgium*
[4]*Groupe Interdisciplinaire de Génoprotéomique Appliquée, Cardiovascular Sciences, University of Liège, Liège, Belgium*
[*]*Corresponding author: Francois Jouret, francois.jouret@chu.ulg.ac.be*
[†]*These authors contributed equally to this work.*

Management of kidney transplant recipients (KTRs) with suspected acute rejection (AR) ultimately relies on kidney biopsy; however, noninvasive tests predicting nonrejection would help avoid unnecessary biopsy. AR involves recruitment of leukocytes avid for fluorodeoxyglucose F^{18} (^{18}F-FDG), thus ^{18}F-FDG positron emission tomography (PET) coupled with computed tomography (CT) may noninvasively distinguish nonrejection from AR. From January 2013 to February 2015, we prospectively performed 32 ^{18}F-FDG PET/CT scans in 31 adult KTRs with suspected AR who underwent transplant biopsy. Biopsies were categorized into four groups: normal ($n = 8$), borderline ($n = 10$), AR ($n = 8$), or other ($n = 6$, including 3 with polyoma BK nephropathy). Estimated GFR was comparable in all groups. PET/CT was performed 201 ± 18 minutes after administration of 3.2 ± 0.2 MBq/kg of ^{18}F-FDG, before any immunosuppression change. Mean standard uptake values (SUVs) of both upper and lower renal poles were measured. Mean SUVs reached 1.5 ± 0.2, 1.6 ± 0.3, 2.9 ± 0.8, and 2.2 ± 1.2 for the normal, borderline, AR, and other groups, respectively. One-way analysis of variance demonstrated a significant difference of mean SUVs among groups. A positive correlation between mean SUV and acute composite Banff score was found, with $r^2 = 0.49$. The area under the receiver operating characteristic curve was 0.93, with 100% sensitivity and 50% specificity using a mean SUV threshold of 1.6. In conclusion, ^{18}F-FDG PET/CT may help noninvasively prevent avoidable transplant biopsies in KTRs with suspected AR.

Abbreviations: ^{18}F-FDG, fluorodeoxyglucose F^{18}; ^{99m}Tc, technetium Tc 99m; ANOVA, analysis of variance; AR, acute rejection; CT, computed tomography; KTR, kidney transplant recipient; PET, positron emission tomography; ROC, receiver operating characteristic; SC, sulfur colloid; SUV, standard uptake value; VOI, volume of interest

Received 10 May 2015, revised 10 June 2015 and accepted for publication 21 June 2015

Introduction

Kidney transplantation currently represents the best available treatment for patients with end-stage renal disease (1); however, its full benefits remain undermined by acute rejection (AR), which may be cellular or antibody mediated (2). Because immunosuppressive drugs treat AR efficiently, an early diagnosis of such a reversible cause of graft failure is essential. In clinical practice, the detection of AR depends critically on assessments of serum creatinine, an insensitive measure of renal injury (3). Ultimately, AR diagnosis relies on renal transplant needle biopsy. Examining kidney samples provides well-characterized and gold standard criteria for renal AR (4); however, such an invasive procedure is associated with a significant risk of bleeding and graft loss and is limited by sampling error and/or interobserver variability (5,6). Moreover, repeated biopsies to evaluate a renal graft's status pose challenges, including practicability and cost. Consequently, other sensitive and less invasive modalities, including gene expression profiling and *omic* analyses of blood and urine samples as well as in vivo imaging, are currently under investigation to reinforce our clinical armamentarium for AR diagnosis (2,7–9). Likewise, it would be useful to noninvasively predict nonrejection in kidney transplant recipients (KTRs) with acute renal dysfunction and suspected AR, thereby avoiding unnecessary transplant biopsy.

Renal AR is associated with recruitment of activated leukocytes into the transplant, and this process is at the basis of the conventional Banff classification (10,11). Activated leukocytes are characterized by high metabolic activity and increased uptake of glucose analog fluorodeoxyglucose F^{18} (^{18}F-FDG), which can be measured by positron emission tomography (PET) (12,13). Hence, ^{18}F-FDG PET is

routinely used for detection, characterization, staging and follow-up of inflammatory processes of various origins (13,14). Moreover, the modern combination of PET with computed tomography (CT) integrates both metabolic and anatomical data and further helps localize and typify tissue inflammation (14). Interestingly, experimental rodent models of allogeneic kidney transplantation suggest that ^{18}F-FDG PET/CT may represent a novel option for detecting renal AR noninvasively, specifically and early (15,16). In the present pilot study, we prospectively assessed the usefulness of ^{18}F-FDG PET/CT imaging in KTRs presenting with suspected AR who underwent a transplant needle biopsy.

Patients and Methods

Patient population and specimens

The study was approved by the institutional review board of the University of Liège (protocol B707201215598). After providing written informed consent, KTRs undergoing a transplant biopsy for suspicion of AR (i.e., increase of serum creatinine levels >30% of baseline value or delayed graft function) (17) between January 2013 and February 2015 were prospectively enrolled. Patients aged <18 years or who were pregnant or breastfeeding were excluded. The management of the patients was based only on the results of renal transplant biopsy and was at the discretion of the clinicians in charge. No data from ^{18}F-FDG PET/CT imaging were available at that time.

Histopathology

Biopsies were assessed by two pathologists blinded to the results of ^{18}F-FDG PET/CT imaging and graded according to the latest Banff criteria (11). Histological lesions were scored as continuous variables (from 0 to 3) on the basis of leukocyte infiltration severity in each component: glomeruli (g), peritubular capillaries (ptc), arteries (v), tubules (t), and interstitium (i). Biopsies diagnosed as normal were defined as having a Banff (i + t) score <2 and no features of a disease process. Biopsies diagnosed as borderline were defined as having a Banff (i + t) score ≥2 (but <i2 − t2 and v = 0), and no feature of a specific disease process. Biopsies diagnosed as AR were defined as having a Banff (i + t) score ≥i2 and ≥t2 and/or v > 0. Biopsies diagnosed as other were defined as showing features of a specific disease process such as polyomavirus BK nephropathy or recurrent or *de novo* glomerular diseases. All biopsies were stained for polyoma BK virus.

^{18}F-FDG PET/CT imaging

The PET/CT procedure was performed using cross-calibrated Philips Gemini TF Big Bore or TF 16 PET/CT systems (Philips Medical Systems, Cleveland, OH) at 201 ± 18 minutes following intravenous injection of a mean dose of 3.2 ± 0.2 MBq/kg of body weight of ^{18}F-FDG. A low-dose helical CT (5-mm slice thickness, 120-kV tube voltage, and 40-mAs tube current–time product) centered to the renal transplant was performed, followed by PET scanning with two bed positions, each lasting 240 seconds. Images were reconstructed using iterative list mode time-of-flight algorithms. Corrections for attenuation, dead time and random and scatter events were applied. The PET/CT procedure was performed within a 48-hour period of the ultrasound-guided renal transplant biopsy under fasting conditions and without administration of contrast agent or diuretics. All ^{18}F-FDG PET/CT scans were done before any modification of immunosuppressive regimens. PET/CT images were read independently by two experienced nuclear medicine physicians blinded to the results of renal transplant biopsies. Four volumes of interest (VOIs) of 1 ml were drawn in the cortical region of both upper (n = 2) and lower (n = 2) poles of the renal transplant, at distance from the pelvicalyceal zone (Figure S1). Additional VOIs were drawn in the lumen of the abdominal aorta (1 ml) and the left psoas muscle (20 ml), which are classically considered as regions of homogeneous baseline ^{18}F-FDG activity. The maximal and mean standard uptake values (SUVs) were measured for each VOI, with no threshold activity, using the following formula: (voxel value in bequerels per milliliter × patient weight in kilograms) / (injected dose in bequerels × 1000 gm/kg).

Statistics

Data were expressed as mean ± 1 standard deviation and as median (minimum–maximum). One-way analysis of variance (ANOVA) and Student *t* tests were performed appropriately using MedCalc software (MedCalc, Mariakerke, Belgium) to statistically compare mean SUVs among groups. A p value <0.05 was considered statistically significant. The correlations between mean SUV and acute composite (g + i + t + v + ptc) Banff scores were performed using MedCalc. Histological lesions were scored as continuous variables (from 0 to 3) on the basis of leukocyte infiltration severity in each component. The receiver operating characteristic (ROC) curve was drawn using MedCalc to discriminate AR group biopsies from nonpathological (normal and borderline groups) biopsies. Sensitivity and specificity were extrapolated from this ROC curve, targeting sensitivity as close to 1 as probable.

Results

From January 2013 to February 2015, 32 ^{18}F-FDG PET/CT scans were performed in 31 KTRs presenting with suspected renal AR, including two with delayed graft function (17). All participants underwent a renal transplant biopsy as part of conventional medical management. Clinical and biological characteristics of the cohort at the time of biopsy are summarized in Table 1. Biopsies were diagnosed as *normal, borderline, AR*, and *other* in 8, 10, 8, and 6 cases, respectively. AR was antibody mediated in only one case, whereas types 1, 2, and 3 cellular AR were found in 5, 1, and 1 case, respectively. The causes of graft failure in the *other* group included immune-allergic interstitial nephropathy (n = 1), polyomavirus BK nephropathy (n = 3), and glomerulonephritis (n = 2). One-way ANOVA did not show any difference in estimated GFR between groups of patients (p = 0.31) (Table 1).

PET/CT imaging was performed within 201 ± 18 minutes after intravenous administration of 3.2 ± 0.2 MBq/kg of body weight of ^{18}F-FDG (Figure 1). Mean glycemia at the time of ^{18}F-FDG injection was 100.8 ± 18.4 mg/dl. One PET/CT procedure was not interpretable because of paravenous injection of ^{18}F-FDG. The mean cumulative exposure dose for PET/CT imaging was 5.41 ± 0.79 mSv. The mean values of SUV from four renal cortical VOIs reached 1.5 ± 0.2, 1.6 ± 0.3, 2.9 ± 0.8, and 2.2 ± 1.2 in histopathological categories normal, borderline, *AR*, and other, respectively (Figure 2A). One-way ANOVA demonstrated a significant difference in mean SUVs among groups (p < 0.01). The mean SUV of biopsy-proven AR was significantly higher than that for normal cases (p < 0.01). There were no significant differences between biopsies with normal

Table 1: Clinical and biological characteristics

		Cohort (n = 32)	Normal (n = 8)	Borderline (n = 10)	Rejection (n = 8)	Other (n = 6)	p value
Recipient	Age (years)	43 (14–66)	25 (20–63)	35 (15–66)	54 (21–66)	57 (43–59)	0.11
	Sex, male/female	24/8	6/2	10/0	4/4	4/2	0.10
	BMI (kg/m^2)	24 ± 5	25 ± 4	24 ± 5	25 ± 6	29 ± 8	0.49
	Dialysis vintage (days)	643 (0–3108)	45 (0–957)	511 (0–2480)	778 (0–3108)	864 (94–1849)	0.06
	PRA maximum (n), <5%/5%–84%/≥85%	29/2/1	8/0/0	10/0/0	5/2/1	6/0/0	0.13
Donor	Donor type (n), DBD/DCD/LD	20/6/6	5/1/2	5/1/4	7/1/0	3/3/0	0.11
	Age (years)	40 (15–65)	33 (25–57)	36 (15–65)	38 (20–58)	46 (15–62)	0.80
	Sex, male/female	15/17	6/2	3/7	3/5	3/3	0.26
	BMI (kg/m^2)	25 ± 5	28 ± 6	24 ± 4	23 ± 1	26 ± 7	0.21
Transplantation	Rank (n), first/second	27/5	5/3	9/1	7/1	6/0	0.23
	Cold ischemic time (min)	585 ± 358	636 ± 394	392 ± 332	798 ± 274	552 ± 349	0.11
	HLA mismatches						
	A	0.9 ± 0.6	0.5 ± 0.5	1.1 ± 0.6	1.0 ± 0.5	0.8 ± 0.4	0.12
	B	1.3 ± 0.6	1.0 ± 0.8	1.3 ± 0.5	1.5 ± 0.5	1.4 ± 0.5	0.40
	DR	0.9 ± 0.7	0.6 ± 0.7	1.1 ± 0.6	0.6 ± 0.7	1.2 ± 0.4	0.20
	Early graft function, immediate/slow/delayed	23/4/5	6/2/0	8/1/1	6/1/1	3/0/3	0.21
Status at the time of biopsy	Maintenance immunosuppression (n)						
	CNI, CsA/FK/none	4/27/1	1/7/0	2/8/0	1/6/1	0/6/0	0.61
	Antimetabolite, MMF/MPA/Aza/none	22/7/1/2	5/2/1/0	7/3/0/0	7/0/0/1	3/2/0/1	0.45
	mTOR inhibitor, yes/no	1/31	0/8	0/10	1/7	0/6	0.37
	Steroids, yes/stop	25/7	7/1	5/5	7/1	6/0	0.07
	Duration of KTx at biopsy (days)	199 (6–5524)	96 (9–5524)	1058 (64–3330)	305 (7–1748)	198 (66–1150)	0.20
	eGFR MDRD (mL/min/1.73 m^2)	40.2 ± 15.5	37.2 ± 15.9	47.3 ± 15.9	38.7 ± 16.2	32.7 ± 10.9	0.31

Data are expressed as mean ± 1 standard deviation and as median (minimum–maximum). Aza, azathioprine; BMI, body mass index; CNI, calcineurin inhibitor; CsA, cyclosporin A; DCD, donor after circulatory death; DBD, donor after brain death; eGFR MDRD, estimated glomerular filtration rate according to the Modification of Diet in Renal Disease formula; FK, tacrolimus; KTx, kidney transplantation; LD, living donor; MMF, mycophenolate mofetyl; MPA, mycophenolic acid; mTOR, mammalian target of rapamycin; PRA, panel reactive antibody.

versus borderline or AR versus other histopathology. Similar observations were made using either maximal SUV from four renal cortical VOI or SUV ratios to aorta or psoas muscle activity (data not shown). Statistical analyses highlighted a positive correlation between mean SUVs and acute composite Banff histological score ($r^2 = 0.49$, $p < 0.0001$) (Figure 2B). Furthermore, increasing grades (from i0 to i3) of leukocyte infiltration in renal allograft interstitium were associated with increasing mean SUVs (from 1.6 ± 0.3 to 2.9 ± 1.1, $p < 0.05$) (Figure 2C).

To further assess the usefulness of ^{18}F-FDG PET/CT in clinical practice, we statistically evaluated the threshold of mean SUVs that would discriminate nonrejection. Indeed, the majority of patients with normal histology or borderline infiltrates will not progress into rejection, whereas instant immunosuppression adjustments are needed in cases of AR (18). Conversely, the diagnosis procedure is specific when polyomavirus BK nephropathy or glomerular diseases are suspected in cases of acute renal failure in KTRs. Consequently, the ROC curve was drawn after distinguishing biopsy-proven AR from normal and borderline histopathology and showed an area under the curve of 0.93 ($p < 0.0001$). Sensitivity and specificity of ^{18}F-FDG PET/CT in diagnosing AR were 100% and 50%, respectively, with a mean SUV threshold of 1.6 (Figure 3). In our cohort, characterized by a 25% prevalence of biopsy-proven AR, the corresponding negative and positive predictive values were 100% and 43.75%, respectively.

Discussion

In the present cohort of 32 ^{18}F-FDG PET/CT procedures performed in 31 KTRs presenting with suspected AR, biopsy-proven AR was characterized by significantly higher ^{18}F-FDG uptake in the renal transplant cortex in comparison to normal biopsies. Mean SUV appeared to be significantly correlated with the severity of leukocyte infiltrates, as assessed by conventional Banff score. Finally, ROC curve analyses suggested that a mean SUV threshold of 1.6 discriminates nonrejection with a negative predictive value of 100%. The poor specificity of ^{18}F-FDG PET/CT in detecting AR is primarily due to the nature of the radiotracer.

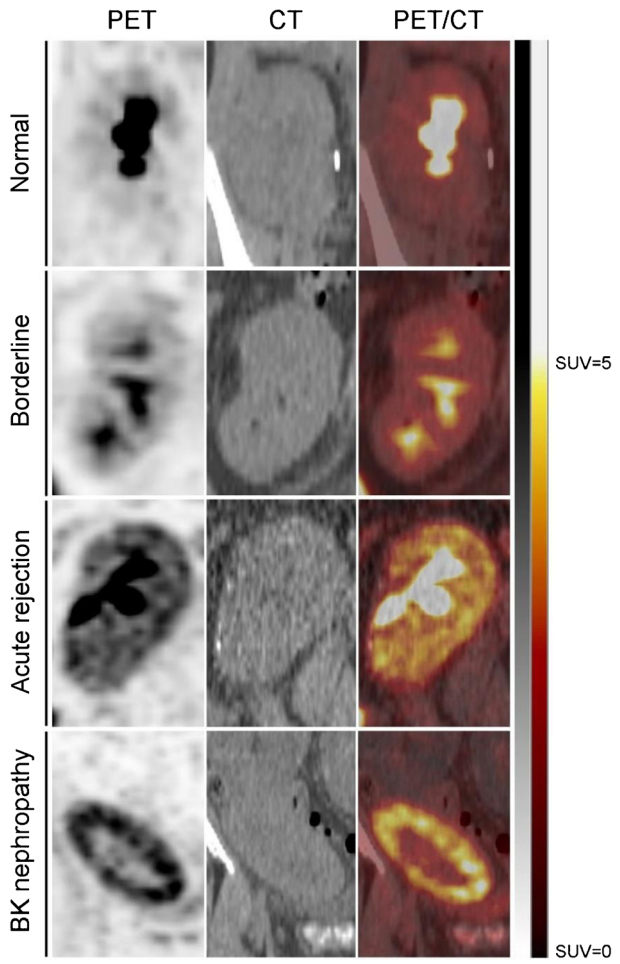

Figure 1: Representative ^{18}F-FDG PET/CT imaging in kidney transplant recipients with suspected acute rejection. PET (left column), CT (middle column), and combined PET/CT images taken after administration of ^{18}F-FDG are shown for kidney transplant recipients with biopsies showing normal histology, borderline changes, acute rejection or polyomavirus BK nephropathy. The arbitrary scale of SUVs (from 0 to 5) is illustrated on the right side. 18F-FDG, fluorodeoxyglucose F^{18}; CT, computed tomography; PET, positron emission tomography; SUV, standard uptake value.

Using radionuclides to image AR is not new and has been performed previously with radiolabeled sulfur colloid (SC) and fibrinogen as well as gallium citrate Ga ^{67}. Comparative meta-analysis suggested a similar specificity of graft labeling during rejection using either radiotracer (19). Still, in clinical settings within the permissible radiation dose, technetium Tc 99m (^{99m}Tc) SC appeared to better discriminate AR on the basis of a strictly visual scale (9). Unfortunately, several studies using computer-assisted quantification of ^{99m}Tc SC uptake by the allograft in comparison to the surrounding pelvis showed conflicting results, with false-negative and -positive rates that were too high to make ^{99m}Tc SC useful in predicting renal AR (20). PET/CT using the glucose analog ^{18}F-FDG has been also proposed for the detection of renal transplant AR in experimental rodent models of allogeneic kidney transplantation (8,15). Inflammatory cells are characterized by a high metabolic status and increased uptake of ^{18}F-FDG (13). The advantages of ^{18}F-FDG PET/CT are rapid imaging, high target:background ratio and direct coregistration with low-dose CT without radiologic contrast medium administration (14). ^{18}F-FDG PET/CT can be used safely in patients with renal function including normal to mildly reduced GFR and end-stage renal disease. In rats, the renal clearance of ^{18}F-FDG does not correlate with renal function (15). In particular, acute kidney injury secondary to cyclosporin exposure or ischemia–reperfusion is not associated with significant elevation of renal ^{18}F-FDG accumulation. There is a surprising gap of knowledge in the literature concerning the impact of acute or chronic kidney injury on renal ^{18}F-FDG uptake in humans. In 2007, Minamimoto et al investigated the influence of renal function on ^{18}F-FDG distribution and uptake in 20 healthy volunteers and 20 patients with suspected renal failure (21). Regions of interest were placed over 15 different regions throughout the body, including the left kidney. No significant difference was observed in renal mean SUVs between healthy volunteers and patients with suspected renal failure. In our series, no difference in estimated GFRs was observed between groups of patients categorized based on kidney histology. Limitations of ^{18}F-FDG PET/CT imaging include its relatively high cost and restricted availability as well as patient exposure to radiation originating from both PET and CT procedures. Still, a cumulative exposure dose of 5.41 ± 0.79 mSv, as observed in this study, remains low in comparison to other classical radiological examinations, such as thorax CT (7mSv), abdomen CT (8 mSv), or coronary angiography (16 mSv) (22). Uptake of ^{18}F-FDG is not specific for inflammation and may be increased in other conditions such as tumors or infections (12,23). Furthermore, physiological urinary excretion of ^{18}F-FDG may hamper the measurement of ^{18}F-FDG uptake in the renal parenchyma (24). To overcome this problem and, eventually, to improve the background:noise ratio, we administered a minimal dose of ^{18}F-FDG and performed late acquisitions. PET/CT images were acquired within 201 ± 18 minutes after intravenous administration of 3.2 ± 0.2 MBq/kg of body weight of the radiotracer. In addition, multiple VOIs were drawn in the renal transplant area, and a mean SUV was considered for statistical analyses. We must admit that we were unable to clearly differentiate the activity of renal parenchyma into medulla- and cortex-related tissue activity. The VOIs were located beneath the renal capsule away from the urinary pelvis, which most probably corresponds to the cortex area. The use of multiple independent VOIs distributed in both the upper and lower renal poles aimed to avert sampling error, which represents a main limitation of transplant biopsy (5,6). Furthermore, assessing ^{18}F-FDG activity in cross-sections by image segmentation software (currently under development and validation) might be another option to minimize the sampling error. Similarly, dynamic or dual/multipoint analysis of ^{18}F-FDG PET/CT imaging may be an interesting way to

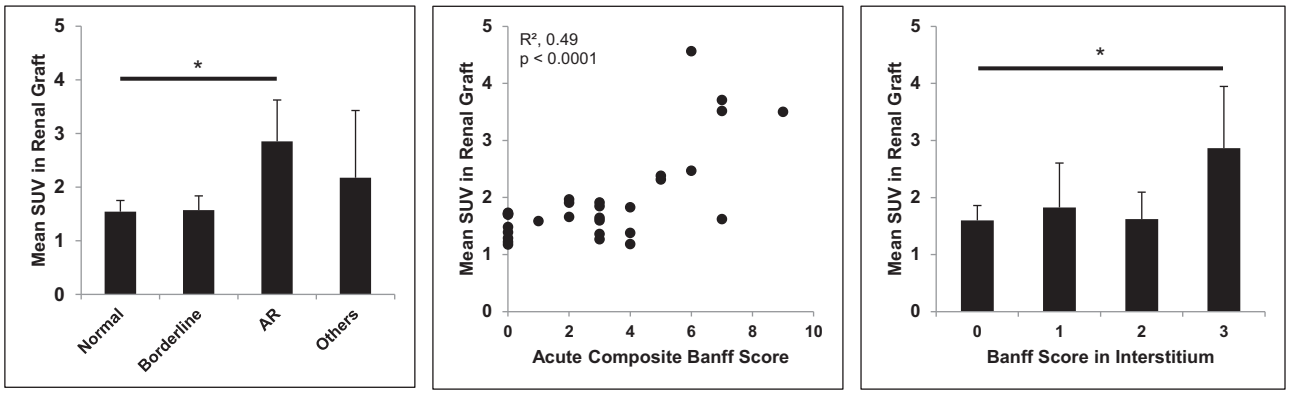

Figure 2: Statistical analyses of fluorodeoxyglucose F^{18} positron emission tomography and computed tomography imaging in kidney transplant recipients with suspected acute rejection. (A) Mean SUVs in kidney transplant recipients with biopsies showing normal histology (n = 8), borderline changes (n = 10), AR (n = 7), or other diagnostics (n = 6). *$p < 0.01$ between normal and AR. (B) Correlation study between mean SUV in renal transplant and acute composite Banff score. (C) Mean SUVs in kidney transplant recipients with biopsies showing increasing Banff score of leukocyte infiltration in the interstitium: grade 0 (n = 13), grade 1 (n = 7), grade 2 (n = 4), and grade 3 (n = 7). *$p < 0.05$ between grade 0 and grade 3. AR, acute rejection; SUV, standard uptake value.

help differentiate between the different pathologies in KTRs presenting with suspected AR (25).

The mean SUV of borderline biopsies was not statistically different from that of normal biopsies, a finding that is in line with recent comparative molecular phenotyping by microarray profiles (26). Similarly, the mean SUV of biopsy-proven AR was not statistically different from that of biopsies showing alternative causes of acute graft dysfunction, including glomerulonephritis and polyomavirus BK nephropathy. The diagnosis procedure, however, is specific when polyomavirus BK nephropathies or glomerular diseases with proteinuria are suspected in cases of acute renal failure in KTRs. The emergence of polyomavirus BK nephropathy coincided with the advent of potent immunosuppressive therapy (27). BK virus infection can occur under all combinations of immunosuppressive therapy, and the beneficial effects of antiviral agents remain unclear. Graft survival in patients with BK virus nephropathy is poor (28). No standardized protocol currently exists for the management of BK viruria or viremia or established BK virus nephropathy. Current clinical practice focuses on screening for BK virus replication in urine and/or blood specimens and preemptive reduction of immunosuppression in viremic patients (29). The Banff Working Proposal 2009, based on viral load and acute tubular injury instead of interstitial inflammation, does not appear to be superior to alternative schemas assessing renal inflammation (30). In our cohort, mean SUV significantly correlated with the severity of graft inflammation and leukocyte infiltration ($r^2 = 0.49$). Furthermore, the Banff score for leukocyte infiltration in renal interstitium was statistically associated with increasing values of mean graft SUV. The ^{18}F-FDG PET/CT pattern, however, was unable to identify the cause of graft inflammation and dysfunction. Ultimately, this determination relies on transplant biopsy examination. The small number of patients did not allow us to compare the uptake of ^{18}F-FDG in cellular versus antibody-mediated AR or in cases of chronic allograft failure. None of the 32 renal transplant biopsies performed in our study showed acute tubular necrosis (ATN). Because no study has investigated the renal uptake of ^{18}F-FDG in cases of ATN in human patients, we must admit that we do not know how ATN would be diagnosed by ^{18}F-FDG PET/CT imaging.

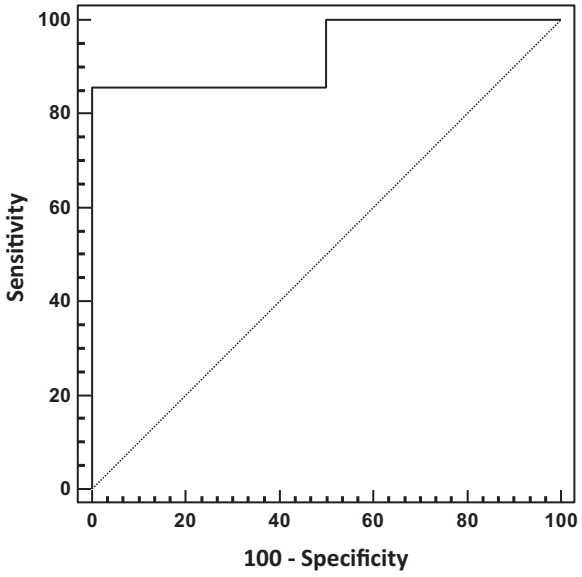

Figure 3: ROC curve using fluorodeoxyglucose F^{18} positron emission tomography and computed tomography imaging in kidney transplant recipients with suspected acute rejection. The ROC curve was drawn after discriminating kidney transplant recipients with biopsies showing or not showing (ie, normal and borderline histology) acute rejection. ROC, receiver operating characteristic.

On the basis of this pilot study, we postulate that ^{18}F-FDG PET/CT imaging may help selected patients avoid undergoing renal transplant biopsy. Our observations are preliminary, given the small number of events and the absence of prospective validation of a mean SUV threshold. Still, the negative predictive value of ^{18}F-FDG PET/CT imaging with a mean SUV threshold at 1.6 reaches 100%, thereby significantly discriminating nonrejection in KTRs presenting with suspected AR. Consequently, transplant needle biopsies may be limited to KTRs in whom ^{18}F-FDG SUV exceeds this threshold. In our series, nine transplant biopsies (28.1%) showing normal (n = 4) or borderline (n = 5) histology were associated with a mean SUV inferior to 1.6. Validation cohorts and additional large prospective series are needed to further test whether a mean SUV threshold for ^{18}F-FDG-PET/CT imaging, in combination with blood and urinary biomarkers (2,7), may help dictate the need for transplant biopsy in KTRs presenting with suspected AR.

Acknowledgments

The authors cordially thank the surgeons (M. Meurisse, C. Coimbra Marques, A. De Roover, O. Detry, E. Hamoir, P. Honoré, L. Kohnen, N. Meurisse, and J-P Squifflet), the physicians (L. Vanovermeire and P. Xhignesse), and the members of the local transplant coordination center (Mme M-H Delbouille, M-H Hans, J Mornard) for their commitment to kidney transplantation at the University of Liège Hospital in Liège, Belgium. We are grateful to P. Delanaye, and C. Ricour for their help with statistical analyses. FJ is a Fellow of the Fonds National de la RechercheScientifique (Research Credit 3309), and received support from the University of Liège (FondsSpéciaux à la Recherche) and from the Fonds Léon Fredericq, as well as from the Royal Academy of Medicine of Belgium (Prix O. Dupont).

Disclosure

The authors of this manuscript have no conflicts of interest to disclose as described by the *American Journal of Transplantation*.

References

1. Tonelli M, Wiebe N, Knoll G, et al. Systematic review: Kidney transplantation compared with dialysis in clinically relevant outcomes. Am J Transplant 2011; 11: 2093–2109.
2. Suthanthiran M, Schwartz JE, Ding R, et al. Urinary-cell mRNA profile and acute cellular rejection in kidney allografts. N Engl J Med 2013; 369: 20–31.
3. Thomas ME, Blaine C, Dawnay A, et al. The definition of acute kidney injury and its use in practice. Kidney Int 2015; 87: 62–73.
4. Williams WW, Taheri D, Tolkoff-Rubin N, Colvin RB. Clinical role of the renal transplant biopsy. Nat Rev Nephrol 2012; 8: 110–121.
5. Furness PN, Taub N. International variation in the interpretation of renal transplant biopsies: Report of the CERTPAP Project. Kidney Int 2001; 60: 1998–2012.
6. Azancot MA, Moreso F, Salcedo M, et al. The reproducibility and predictive value on outcome of renal biopsies from expanded criteria donors. Kidney Int 2014; 85: 1161–1168.
7. Ong S, Mannon RB. Genomic and proteomic fingerprints of acute rejection in peripheral blood and urine. Transplant Rev (Orlando) 2015; 29: 60–67.
8. Pawelski H, Schnockel U, Kentrup D, Grabner A, Schafers M, Reuter S. SPECT- and PET-based approaches for noninvasive diagnosis of acute renal allograft rejection. BioMed Res Int 2014; 2014: 874785.
9. Einollahi B, Bakhtiari P, Simforoosh N, et al. Renal allograft accumulation of technetium-99m sulfur colloid as a predictor of graft rejection. Transplant Proc 2005; 37: 2973–2975.
10. Sarwal M, Chua MS, Kambham N, et al. Molecular heterogeneity in acute renal allograft rejection identified by DNA microarray profiling. N Engl J Med 2003; 349: 125–138.
11. Haas M, Sis B, Racusen LC, et al. Banff 2013 meeting report: Inclusion of c4d-negative antibody-mediated rejection and antibody-associated arterial lesions. Am J Transplant 2014; 14: 272–283.
12. Jouret F, Lhommel R, Beguin C, et al. Positron-emission computed tomography in cyst infection diagnosis in patients with autosomal dominant polycystic kidney disease. Clin J Am Soc Nephrol 2011; 6: 1644–1650.
13. Keidar Z, Gurman-Balbir A, Gaitini D, Israel O. Fever of unknown origin: The role of 18F-FDG PET/CT. J Nucl Med 2008; 49: 1980–1985.
14. Boellaard R, Delgado-Bolton R, Oyen WJ, et al. FDG PET/CT: EANM procedure guidelines for tumour imaging: Version 2.0. Eur J Nucl Med Mol Imaging 2015; 42: 328–354.
15. Reuter S, Schnockel U, Schroter R, et al. Non-invasive imaging of acute renal allograft rejection in rats using small animal F-FDG-PET. PLoS One 2009; 4: e5296.
16. Grabner A, Kentrup D, Schnockel U, et al. Non-invasive imaging of acute allograft rejection after rat renal transplantation using 18F-FDG PET. J Vis Exp 2013: e4240.
17. Mallon DH, Summers DM, Bradley JA, Pettigrew GJ. Defining delayed graft function after renal transplantation: Simplest is best. Transplantation 2013; 96: 885–889.
18. Beimler J, Zeier M. Borderline rejection after renal transplantation-to treat or not to treat. Clin Transplant 2009; 23(Suppl 21): 19–25.
19. George EA, Codd JE, Newton WT, Haibach H, Donati RM. Comparative evaluation of renal transplant rejection with radioiodinated fibrinogen 99mTc-sulfur collid, and 67Ga-citrate. J Nucl Med 1976; 17: 175–180.
20. Smith SB, Wombolt DG. Histologic correlation of transplant rejection diagnosed by computer-assisted sulfur colloid scan. Urology 1983; 21: 151–153.
21. Minamimoto R, Takahashi N, Inoue T. FDG-PET of patients with suspected renal failure: Standardized uptake values in normal tissues. Ann Nucl Med 2007; 21: 217–222.
22. Mettler FA Jr, Huda W, Yoshizumi TT, Mahesh M. Effective doses in radiology and diagnostic nuclear medicine: A catalog. Radiology 2008; 248: 254–263.
23. Barrington SF, Mikhaeel NG, Kostakoglu L, et al. Role of imaging in the staging and response assessment of lymphoma: Consensus of the International Conference on Malignant Lymphomas Imaging Working Group. J Clin Oncol 2014; 32: 3048–3058.
24. Engel H, Steinert H, Buck A, Berthold T, Huch Boni RA, von Schulthess GK. Whole-body PET: Physiological and artifactual fluorodeoxyglucose accumulations. J Nucl Med 1996; 37: 441–446.
25. Hustinx R, Smith RJ, Benard F, et al. Dual time point fluorine-18 fluorodeoxyglucose positron emission tomography: A potential method to differentiate malignancy from inflammation and

normal tissue in the head and neck. Eur J Nucl Med 1999; 26: 1345–1348.

26. de Freitas DG, Sellares J, Mengel M, et al. The nature of biopsies with ''borderline rejection'' and prospects for eliminating this category. Am J Transplant 2012; 12: 191–201.
27. Pham PT, Schaenman J, Pham PC. BK virus infection following kidney transplantation: An overview of risk factors, screening strategies, and therapeutic interventions. Curr Opin Organ Transplant 2014; 19: 401–412.
28. Masutani K. Current problems in screening, diagnosis and treatment of polyomavirus BK nephropathy. Nephrology 2014; 19(Suppl 3): 11–16.
29. Costa C, Cavallo R. Polyomavirus-associated nephropathy. World J Transplant 2012; 2: 84–94.
30. Masutani K, Shapiro R, Basu A, Tan H, Wijkstrom M, Randhawa P. The Banff 2009 Working Proposal for polyomavirus nephropathy: A critical evaluation of its utility as a determinant of clinical outcome. Am J Transplant 2012; 12: 907–918.

Supporting Information

Additional Supporting Information may be found in the online version of this article.

Figure S1: Representative analysis a fluorodeoxyglucose F 18 positron emission tomography and computed tomography image in a kidney transplant recipient with suspected acute rejection. Four 1-ml VOIs (white circles) are drawn in the cortex area of both upper and lower poles of the renal transplant. Maximal and mean standard uptake values (SUVs) are independently measured in each VOI. In the present case, maximal SUVs in VOIs 1–4 were 1.88, 1.71, 1.52 and 1.55, respectively, whereas mean SUVs in VOIs 1–4 were 1.41, 1.32, 1.44, and 1.41, respectively. The biopsy of this patient showed normal histology. VOI, volume of interest.